

Flight Performance of the Stabilization System of the Communications Technology Satellite

F.R. Vigneron* and R.A. Millar†

Communications Research Center, Department of Communications, Ottawa, Canada

Flight performance for the three-axis stabilized earth-pointing mode of the Communications Technology Satellite is described. The operational environment and flight performance are demonstrated to be in accord with projections made prior to flight. Performance is within the limits required for efficient satellite communications. No adverse structural flexibility/control system interactions are evidenced. Performance and life data on components have been favorable to date, although a temporary malfunction of an earth sensor has been experienced. Spacecraft stabilization during momentum dumping, sun and moon interference, and E-W stationkeeping are illustrated. The automatic failure-protect mode has been demonstrated to operate successfully.

Introduction

THE attitude control subsystem of the Communications Technology Satellite (CTS)‡ operates during three distinct phases associated with the spacecraft's mission. These phases are the spin-stabilized phase which begins in transfer orbit and proceeds to synchronous orbit station acquisition; the ground-controlled phase which involves conversion from spin-stabilization to three-axis stabilization; and, finally, the three-axis stabilized phase which entails accurate uninterrupted Earth pointing with on-spacecraft automatic hardware for a design life that exceeds two years.

The CTS was launched and injected into transfer orbit on Jan. 17, 1976. The ground-controlled conversion to the three-axis stabilized phase was achieved during Jan. 31, and Feb. 1, 1976. The on-spacecraft automatic three-axis stabilization system was activated on Feb. 1, 1976.

This paper presents a description of the system, flight performance, and flight experience for the three-axis stabilized phase. Flight performance of the hydrazine reaction control subsystem (RCS), the ground-controlled conversion to the three-axis stabilized phase, the deployable solar array, and other subsystems of the CTS are discussed in Refs. 1-5.

Description of Three-Axis Stabilization System

The CTS configuration in the three-axis stabilized synchronous orbit state is shown in Fig. 1. The spacecraft is a tri-spin body about pitch—the spacecraft's central body tracks the Earth using automatic control and hence rotates once per day; the momentum wheel rotates at approximately 4000 rpm with respect to the central body; the solar array is sun-oriented (by automatic sun-tracking or by clock mode) and is essentially nonrotating with respect to an inertial reference frame. The hardware components required for three-axis stabilization, namely the two nonspinning earth sensor assemblies (NESA-A and NESA-B), the momentum wheel, the attitude control electronics assembly (ACEA), and the thrusters are shown in Fig. 1.

Because of the particular mass and stiffness properties of this configuration, the spacecraft dynamics uncouple into independent and separate classes of motion. One class includes angular motions about the pitch axis and symmetric array deformations. Another class includes angular motion about the roll and yaw axes and antisymmetric array deformations. This basic uncoupling has been used to advantage, in that the pitch axis and roll/yaw axes controllers have been designed independently. Flight performance has borne out the soundness of this premise. Accordingly, pitch and roll/yaw stabilization systems will be discussed separately.

References 6 and 7 provide a description of the expected environment and the design and hardware configuration as

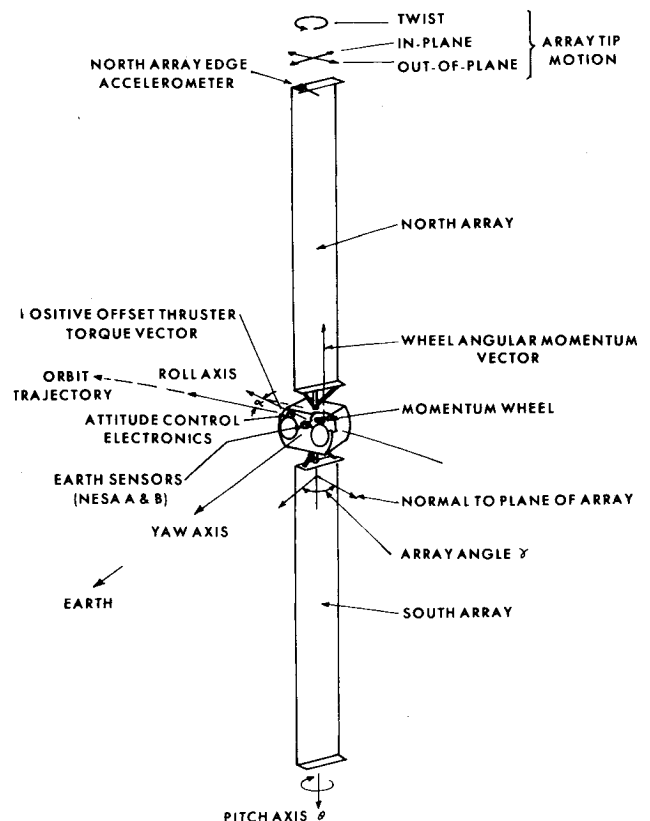


Fig. 1 CTS on orbit state.

Presented as Paper 77-1059 at the AIAA 1977 Guidance and Control Conference, Hollywood, Fla., Aug. 8-10, 1977; submitted Nov. 9, 1977; revision received April 25, 1978. Copyright © American Institute of Aeronautics and Astronautics, Inc., 1977. All rights reserved.

Index categories: Spacecraft Dynamics and Control; Spacecraft Testing, Flight and Ground.

*Research Scientist. Member AIAA.

†Research Engineer.

‡CTS is also known as Hermes.

planned in 1972-1974. The following subsections provide a brief description of the system as manufactured and flown.

Pitch Control

The pitch control loop is shown in Fig. 2. The pitch controller is of the linear proportional-integral-derivative (PID) type, and utilizes a pulsewidth modulator driven momentum wheel as its torque actuator. The pitch thrusters can be activated by ground command for wheel momentum dumping. A functional description and stability analysis of the loop are presented in Ref. 8.

Automatic Failure Protection (AFP)

The dynamic state with the momentum wheel driven at constant speed and with pitch body rate below a certain value is a stable holding state. The basic idea of AFP is to put the spacecraft into this dynamic state automatically, in the event of a failed PID controller, a stuck-on thruster, a failed Earth sensor, or certain types of power failure.

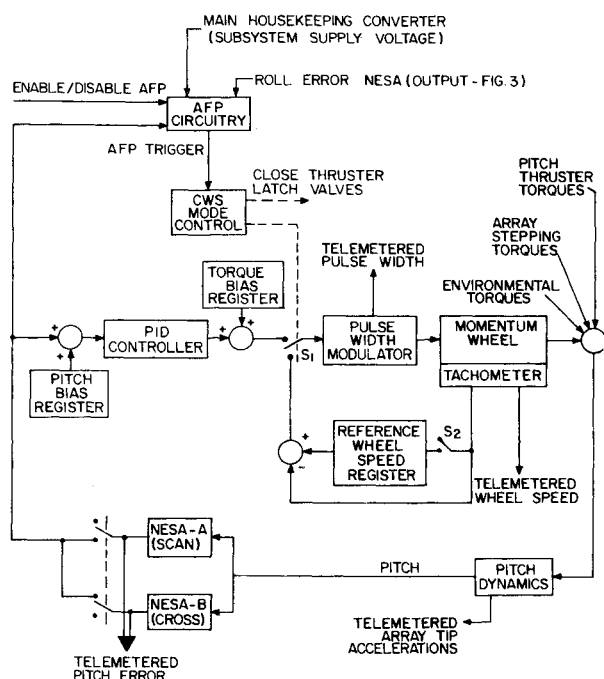


Fig. 2 Pitch control loop.

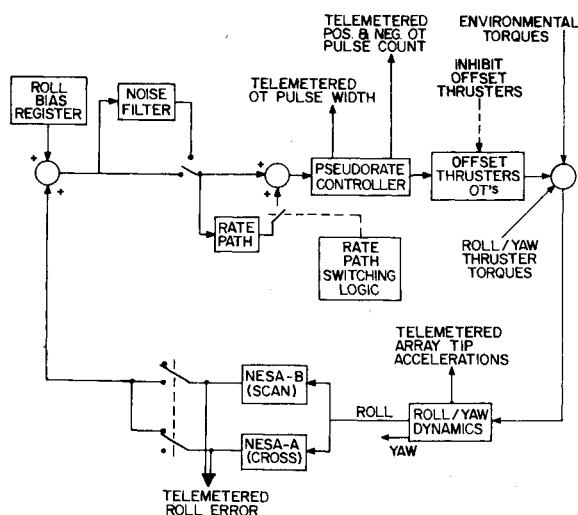


Fig. 3 Roll/yaw control loop.

Tachometer feedback around the pulsewidth modulator and wheel provides the desired constant wheel speed (CWS) mode.

AFP will automatically switch in if any of the following events occur: 1) roll or pitch exceeds the full scale of the NESA (approximately 2.8 deg.); 2) loss of subsystem supply voltage; and 3) loss of Earth presence (flag). AFP, when triggered, automatically causes the following spacecraft switchings: 1) switch from prime to redundant ACEA; 2) switch to redundant momentum wheel power converter; 3) switch from PID controller to CWS controller; and 4) close all RCS latch valves. AFP recovery may be made by uncomplicated ground-based procedures.

Roll and Yaw Control

The roll/yaw control loop is shown in Fig. 3. Stabilization is based on the momentum bias (gyroscopic stiffness) principle, employing a single wheel mounted with its rotor axis fixed parallel to the spacecraft pitch axis. Roll and yaw error trim is achieved by operation of either a positive or negative offset thrust engine in response to detected roll errors. The thrusters produce a torque about the roll and yaw axes simultaneously. The torque causes an appropriate realignment of the angular momentum, which tends to null both roll and yaw errors.

The roll/yaw controller is basically a dual time constant pseudorate controller with rate augmentation. The rate path provides offset thruster pulses which eliminate potential limit cycle behavior.⁹

To optimize fuel usage over the mission, a roll error noise filter can be switched in or out, and pseudorate parameter sets can be selected via ground command.

Hardware and Weight

The system employs two infrared scan-type nonspinning Earth sensors—NESA-A and NESA-B. NESA-A scans east-west and is boresighted 3.5 deg below the equatorial plane; NESA-B scans north-south and is boresighted at 3.5 deg west from the Earth's center. Earth NESA generates an angular reading from its Earth scan information and from its viewed Earth chord (cross-scan) information. The type of NESA used on CTS is described in Ref. 10. The two NESAs are boresighted so that they will not experience sun (or moon) interference at the same time. Switching between NESAs to

Table 1 Stabilization and control components

Component	Weight, lb	Major parameters
Components used for on-orbit stabilization		
Earth sensors, NESA-A and B	11.2	Field of view = ± 26.5 deg Sensing range = ± 2.8 deg Accuracy = ± 0.05 deg
Attitude control electronics assembly	11.9	
Momentum wheel	17.3	Momentum 15 ft-lb-s at 3750 rpm
Additional components for transfer orbit and acquisition		
Sun sensor—Nonspinning	5.9	± 1 deg over 4π steradian FOV
—Spinning		± 0.225 deg in a 0.1×64 deg FOV
Spinning Earth sensor	3.0	Accuracy ± 0.1 deg at 60 rpm
Nutation damper	0.8	
Three axis rate gyro	2.5	Null accuracy ± 12 deg/s Dynamic Range ± 10 deg/s
Wiring harness	1.8	
Total weight of system	54.4	
Other		
Reaction control system tanks and hardware	39.6	

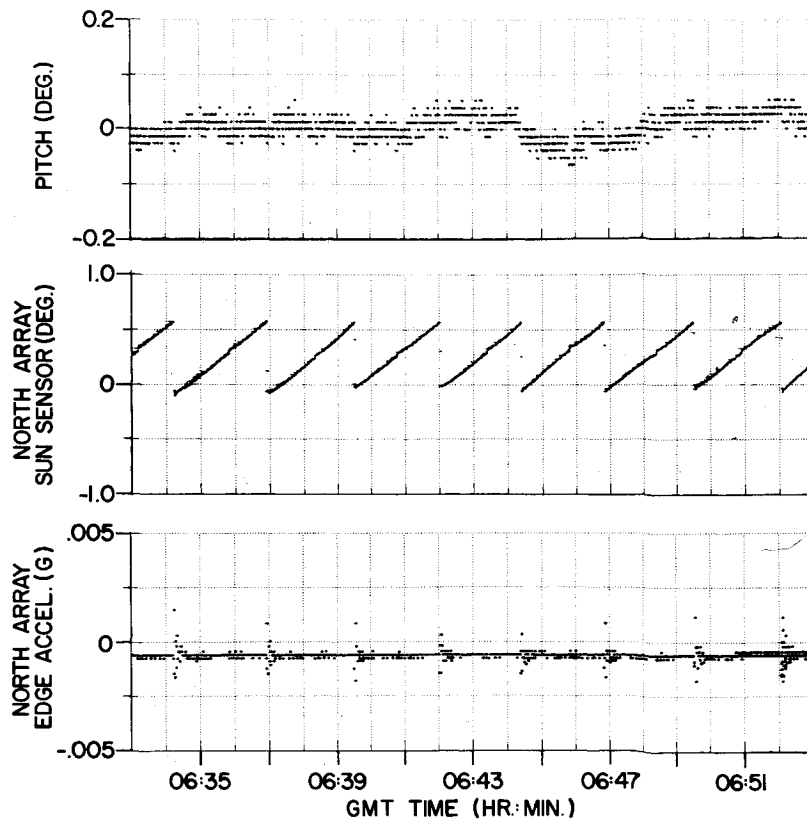


Fig. 4 Steady-state pitch operation—day 281, 1976.

avoid sun and moon interference is done by ground command on the basis of computer-generated predictions.

The CTS momentum wheel has a nominal stored momentum and speed of 15 ft-lb-s and 3750 rpm, respectively. The CTS wheel is described in Ref. 11. The reader is referred to Ref. 1 for a discussion of the hydrazine thruster system. The ACEA uses digital signal processing and low-power TTL circuitry.

The weight of the subsystem is given in Table 1.

Performance Results, Pitch Stabilization

Pitch Controller Performance

Typical data taken during steady-state pitch operation are shown in Fig. 4. The controller holds the sensed error to within ± 0.03 deg, as shown when controlling from the scan channel. The sun sensor and accelerometer traces illustrate array sun-tracking operation. Pitch, as measured from the cross channel, has slightly more sensor-induced noise. Data generated by digital simulation of the loop shown in Fig. 2 show close correspondence to the flight data of Fig. 4.

Each time the array drive and track steps the nominal 0.6 deg, the array twists and bends a small amount, as is evidenced by the north array edge accelerometer trace. The accelerometer transient represents a twist deformation of about 0.5 deg and damps out between array steps. Structural nonrigidity, although in evidence in this form, does not interact or interfere with the operation of the pitch or array stepping controllers.

Momentum Wheel Speed Change and Pitch Axis External Torque

The momentum wheel speed changes daily, as shown in Fig. 5. The change is due to external torque about the pitch axis. The torque, L , derived from $L = J\dot{\Omega}$, is approximated by

$$L = A + B \sin \omega_o t \quad (1)$$

J is the moment of inertia of the wheel, Ω is the speed of the wheel, and ω_o equals 1 rev/day (the orbit frequency). For the

data of Fig. 5, $A = 0.088 \times 10^{-5}$ ft-lb and $B = 0.058 \times 10^{-5}$ ft-lb.

The torque is induced mainly by solar pressure and is due to the center of pressure of the arrays being offset from the center of mass of the spacecraft, as a result of in-plane and out-of-plane array bending deformations and alignments (the offsets also change as the array rotates with respect to the spacecraft).

A and B may be expected to vary with change in sun angle relative to the pitch axis (± 23.5 deg over the course of a year). The data bear this out, but this aspect of performance has yet to be analyzed in detail.

Pitch Disturbance from Momentum Wheel Bearing Drag Variations

During the first 10 days of the mission, occasional pitch error transients, of the type illustrated in Fig. 6 were observed. Pitch deviated from its usual ± 0.03 deg accuracy up to 0.20 deg over a period of 2-3 min. The momentum wheel controller pulsewidth (i.e., power into the wheel) also experienced a small step increase. The number of times that the transient was observed per day is shown in Fig. 7. After about 10 days, the occurrence of the transients lessened.

It has been established that the behavior indicated in Fig. 6 is caused by an occasional abrupt increase in bearing drag torque of about 5%. Simulation of a bearing drag torque increase verifies the observed performance. The drag torque variations could be caused by a change in lubricant distribution from time to time, or by bearing retainer ring instability and vibration. Drag torque variations have been observed in wheels under ground-based life test.

On the basis of Fig. 7 and observations to date, it is believed that the wheel bearings underwent a period of wear-in and adjustment to the 0g environment (accompanied by drag torque variations), and, since March 1976, have reached a relatively stable state where drag torque variations occur much less often. Pitch transients greater than 0.1 deg due to drag torque variations have occurred only a few times since (e.g., days 175 and 241, 1976).

Fig. 5 Daily wheel speed variation.

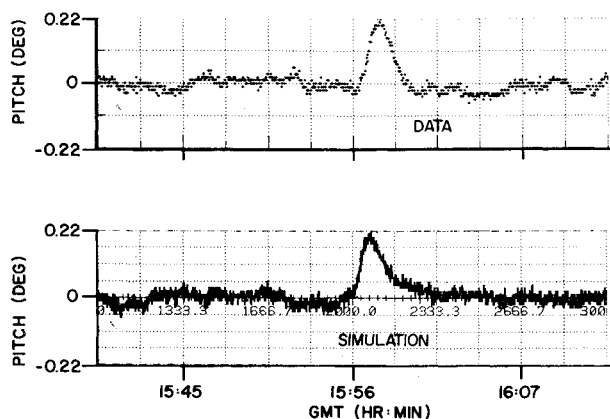
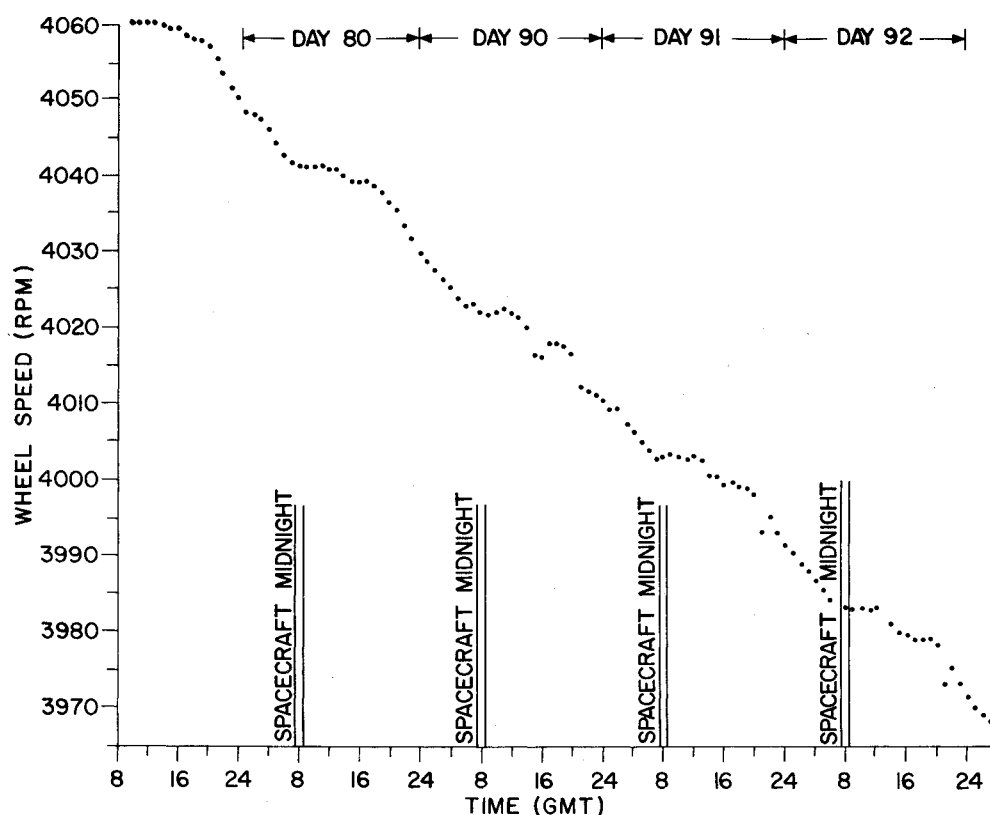


Fig. 6 Typical and simulated pitch transient on day 40, 1976.

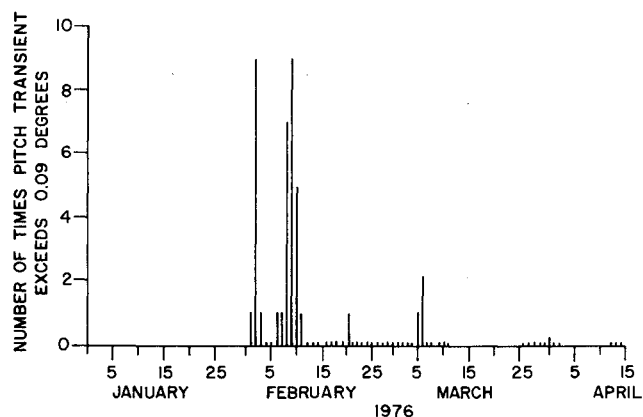
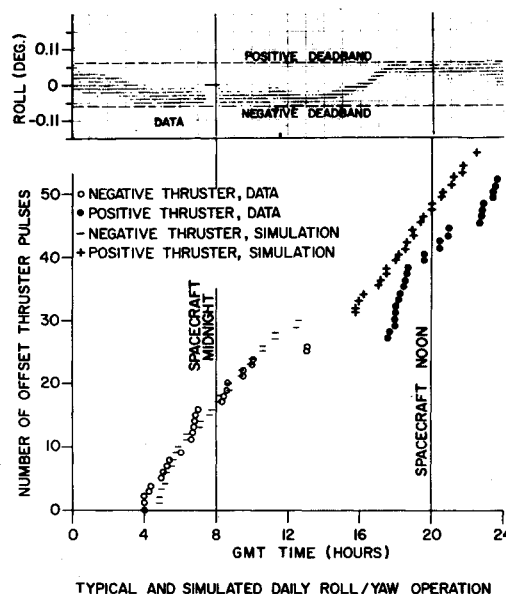


Fig. 7 Histogram of pitch transient.

Fig. 8 Typical and simulated daily roll/yaw operation—day 53, 1976 (simulation assumes a solar torque of 0.5×10^{-5} ft-lb).

Comparison of flight and ground test data for wheel spin-up and steady-state operation show that the wheel has not changed its basic characteristics as a result of launch and 0g operation. Currently, there is no concern regarding the mission life of the wheel.

Performance Results, Roll/Yaw Stabilization

Roll/Yaw Controller Performance

Data taken during steady-state operation of the roll/yaw controller are shown in Figs. 8 and 9. In Fig. 8, flight data and simulation results for offset thruster operation are compared for a 24-h time period. The roll error signal is held within its deadband of ± 0.06 deg by the controller. Both positive and

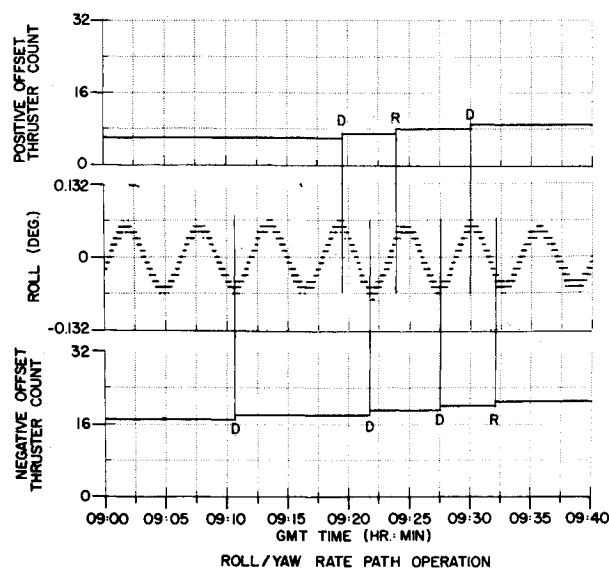


Fig. 9 Roll/yaw operation—day 258, 1976 (shows nutation period and rate path operation).

negative offset thrusters operate in accordance with the external solar torque environment. Simulation results, which show agreement with the data, indicate that the yaw error remained within ± 0.35 deg during this particular day.

Figure 9 shows details of roll error data and offset thruster activity on day 258, 1976, when the nutation angle was comparable with the deadband. The controller holds the roll error to within the deadband and suppresses the tendency to limit cycle. The spacecraft's gyroscopic nutation period of 329 s is evident. The nutation period T , calculated from the formula

$$T = 2\pi\sqrt{I_x I_z} / (J\Omega) \quad (2)$$

agrees with the observed data. In Eq. (2), I_z and I_x are the spacecraft's moments of inertia about yaw and roll, and $J\Omega$ is the stored angular momentum of the wheel. The offset thrusters are noted to respond to a roll signal which slightly exceeds the deadband (D pulse). A rate path initiated pulse (R pulse), which maintains the nutation at less than deadband limits, is seen to follow the D pulse by about 300 s. The R pulse (of the same sign as the D pulse) will fire, provided that the roll angle is less than the deadband, the sum of roll angle and derived roll rate exceeds the deadband, and less than 300 s have elapsed since a D pulse. The numbers (300-s cutoff, deadband, etc.) are based on prelaunch expectation of performance and are hardwired in the ACEA. Valid operation is dependent on the spacecraft nutation period T being between about 270–370 s. Since T depends on wheel speed, as per Eq. (2), correct rate path operation thus necessitates that wheel speed be maintained between limits which insure $270 \leq T \leq 370$. CTS is operated between wheel speed limits of 3800 and 4300 rpm; these bounds conform with acceptable rate path performance. CTS has been operated at 3580–3700 rpm, and, in this range, the R pulse is suppressed because T becomes too large with respect to the 300-s cutoff. Under these conditions, the system was observed to develop a stable deadband-to-deadband limit cycle sustained by alternate offset thruster firings.

Earth capture and response of the system to external disturbances are found to be in accordance with prelaunch expectations and agree with simulation results. Roll errors settle to within the deadband in about 10 min; yaw errors settle to steady state within 3–4 h.

External Torque About Roll and Yaw

The external torque derived from offset thruster firing history is shown in Fig. 10. The torque may be attributed

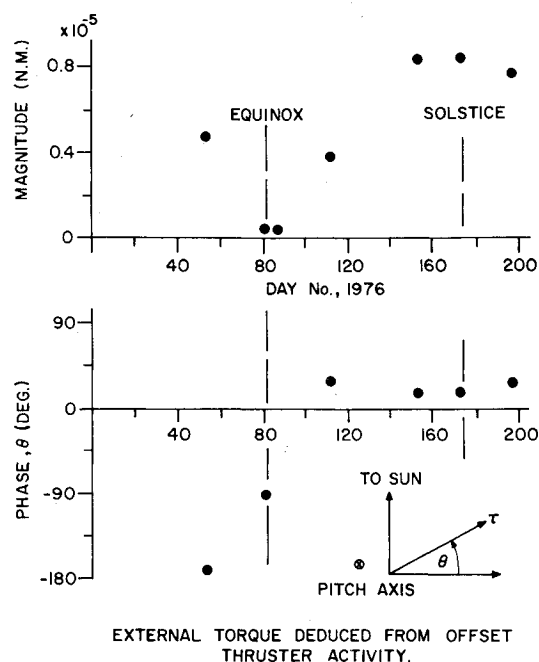


Fig. 10 External torque deduced from offset thruster operation.

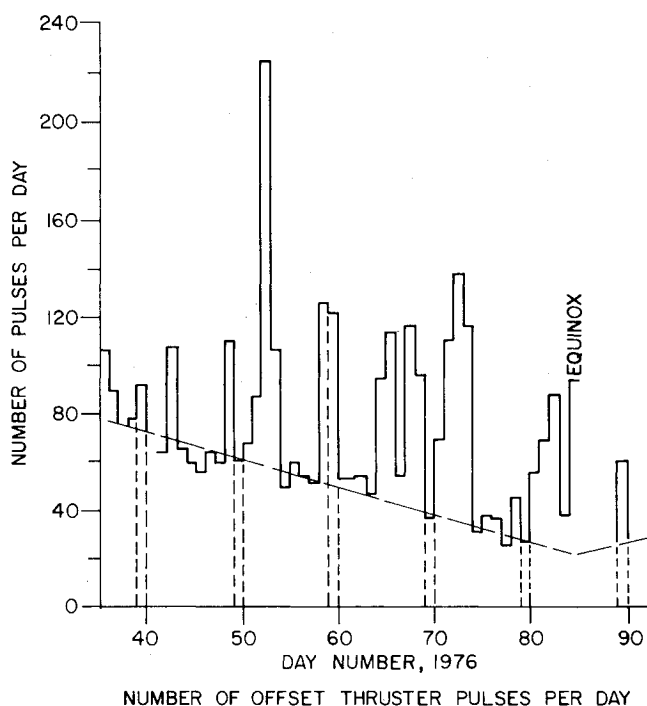


Fig. 11 Fuel consumption per day, offset thrusters.

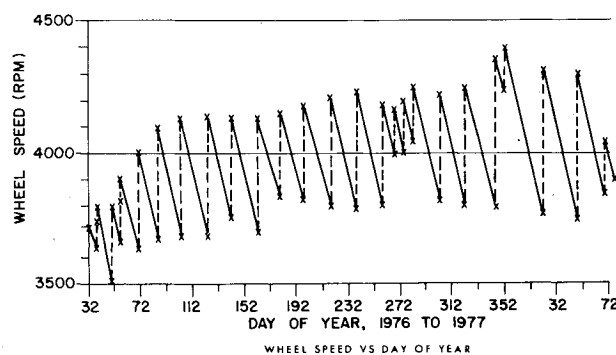


Fig. 12 Wheel speed vs day of year.

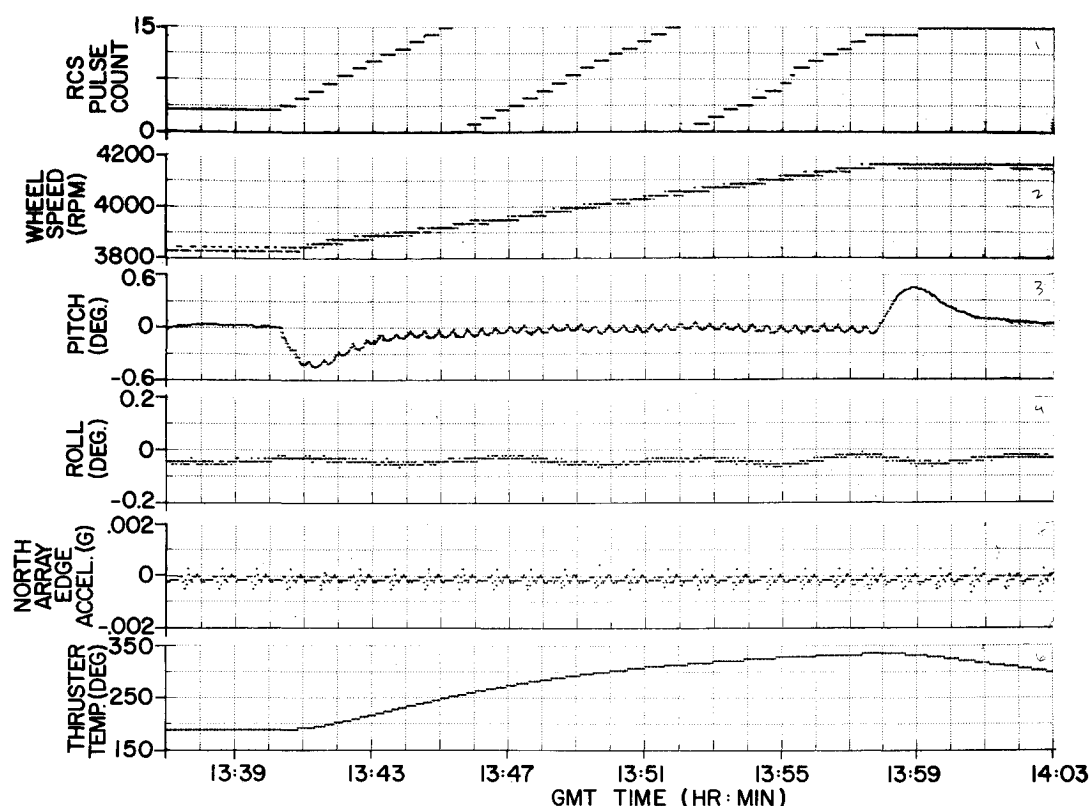


Fig. 13 Momentum dump day 180, 1976 – 50 ms pulse width, 28 pulses of pitch thruster 25 s apart, and 2 offset thruster pulses, 0.0018 lb fuel consumed.

primarily to the effect of solar pressure on the solar array. The component normal to the sun line is due to the dihedral effect, and the component parallel to the sun line is caused by the propeller effect.^{3,7} There is no evidence of torque attributable to the Earth's magnetic field.

Offset Thruster Fuel Consumption

Fig. 11 summarizes offset thruster activity between days 32 and 87, 1976. The fuel per pulse is about 3.2×10^{-5} lbm. The delivered impulse is due to: 1) reaction to external solar torque; 2) reaction to misalignment of the NESAs with respect to the momentum wheel, and roll/yaw disturbances induced by NESAs switchings, array slewing, momentum dumping, and E-W stationkeeping; and 3) limit cycle operation in instances where the wheel speed is sufficiently low that the rate path R pulses are suppressed.

The dashed line in Fig. 11 indicates the number of pulses observed on quiet days when 1 and 2 are minimal. At equinox, 1 is zero, thus, the contribution due to 2 during quiet days is 20-25 pulses. The large peaks above the dashed lines, due primarily to 3, have been reduced beyond day 90, 1976, by raising wheel speed limits to 3800-4300 rpm. The fuel usage for offset thruster operation for CTS is about 0.6 lbm/yr. Fuel consumption for this mission is discussed in Ref. 1.

Stabilization System Performance During Geosynchronous Orbit Events

Momentum dumping, E-W stationkeeping, sun and moon interference avoidance, and eclipse traverse are housekeeping operations performed on CTS. N-S stationkeeping is not a requirement.

Momentum Dumping

Wheel speed vs day of year for 1976 is shown in Fig. 12. A momentum dump is required about every 25 days to compensate for wheel speed change due to solar torque and E-W stationkeeping disturbances.

Momentum dumping is done by ground command, which applies a pitch torque to the spacecraft. Pitch and roll/yaw pointing are maintained by the onboard control loops shown in Figs. 2 and 3. A typical momentum dump is shown in Fig. 13. It is noted that pitch angle is maintained to within ± 0.5 deg, and roll disturbances are almost non-existent. The ± 0.5 deg pitch disturbance is a function of the duty cycle and pulsewidth of the pitch thruster, and can be made less at the expense of taking longer to do the momentum dump. Momentum dumping does not induce significant array accelerations. The observed acceleration transients are due to normal array stepping.

There have been anomalies with a pitch thruster (P_1) where the expected impulse does not agree with the delivered impulse. During some momentum dumps, response from three to five commanded pulses was not observed. The cause of this anomaly has not been conclusively identified.

East-West Stationkeeping

Stationkeeping is required every 25-35 days to maintain longitude within ± 0.2 deg. Stationkeeping is done by ground command of either an east or a west thruster. Attitude stabilization is maintained by the onboard control loops. Attitude control system response to a typical stationkeep is shown in Fig. 14. Pitch and roll are maintained to within ± 0.13 and ± 0.09 deg, respectively, in this instance.

Sun Interference

Operation during a sun interference is shown in Fig. 15. In this instance, the sun interferes with NESAs-B, but not with NESAs-A. NESAs-B roll and pitch data are made invalid by the sun.

CTS procedure is to avoid operation with invalid pitch data by switching sensors (i.e., choosing NESAs-A scan or NESAs-B cross) as appropriate to insure that valid attitude information is fed to the controller. Switching is done by ground command in advance of interference. A small pitch perturbation

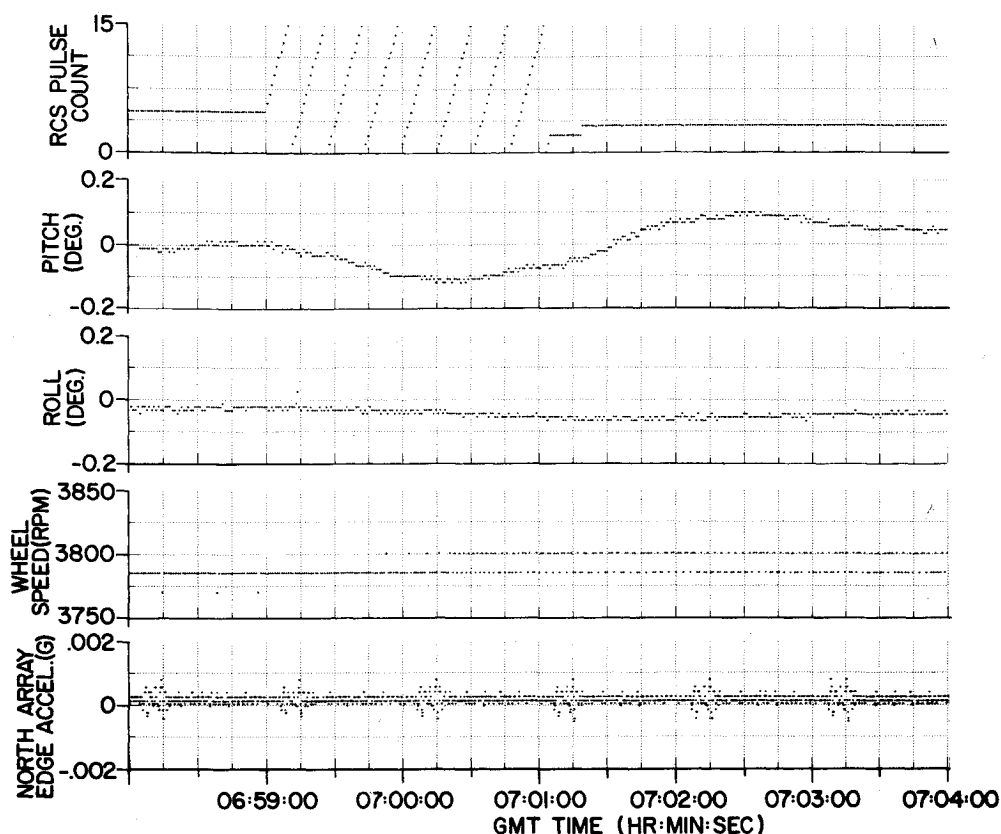


Fig. 14 E-W stationkeep, day 239, 1976. 125 pulses of west engine, 1 s apart $\Delta V = 1.7647$ cm/s, 0.0076 lb fuel, 1 offset thruster pulse.

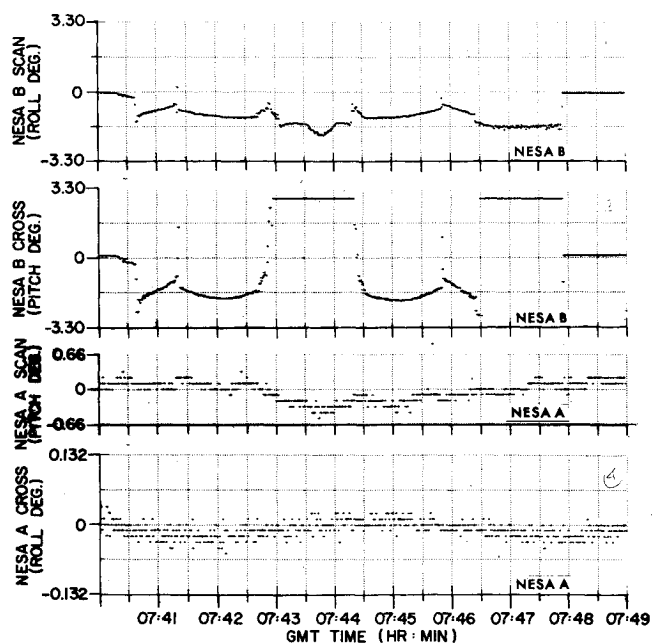


Fig. 15 Sun interference on NESA-B day 054, 1976.

(usually less than 0.05 deg) is observed at the time of sensor switch, as the system gives up one sensor and captures with the other. (The sensors have a slow-varying relative misalignment discussed in a later section.)

CTS procedure is to avoid roll/yaw operation with invalid roll data by inhibiting offset thruster firing and coasting through the short periods of interference, using the momentum wheel's gyroscopic stiffness for stabilization. The offset thrusters are inhibited by ground command in advance of interference for a period of about 30 min during this

operation. Roll and pitch errors are maintained within ± 0.1 deg.

Moon Interference

Moon interference with either NESA will result in invalid data in a manner similar to that experienced in sun interference, but to a lesser degree (e.g., induced NESA-B errors of ± 0.5 deg in pitch and ± 1.4 deg in roll over a duration of 2 min). During NESA-B interference, invalid roll data are avoided by inhibiting the offset thrusters as per the sun avoidance procedure, and the pitch controller operates using NESA-A without loss of Earth lock. Moon interference with NESA-A can be accommodated by switching NESA-A off and allowing NESA-B to control pitch.

Traversal Through Eclipse

Although eclipse traversal does not directly influence stabilization system operation, the following perturbations are experienced.

- 1) The array stepping is stopped prior to eclipse to conserve spacecraft power. Immediately after eclipse, the arrays are switched into sun-track mode and slew by as much as 17 deg to recapture the sun. The slew produces a perturbation in pitch up to 0.5 deg over a few minutes and in roll up to 0.03 deg.
 - 2) The spacecraft experiences a small thermal-induced structural shock which changes the nutation amplitude by a small amount.
 - 3) The alignment of the NESAs changes with respect to the spacecraft principal axes and momentum wheel vector by small amounts.
- The latter two perturbations are handled by the stabilization system without significant deviation in attitude. They are discussed further under "Attitude Drift and Recapture Test" and "Pointing Accuracy."

Table 2 Pointing errors associated with control system

	Normal mode, ^a deg			Momentum dump, deg			E-W stationkeep deg		
	Pitch	Roll	Yaw	Pitch	Roll	Yaw	Pitch	Roll	Yaw
Alignment/stability of NESA	±0.08	±0.08		±0.08	±0.08		±0.08	±0.08	
Alignment of momentum wheel			0.05			0.05			0.05
Stabilization system null error	±0.04	±0.06	±0.5	±0.6	±0.07	±0.5	±0.1	±0.09	±0.5
Pointing error at antenna base (rss of above)	±0.09	±0.1	±0.5	+0.6	±0.11	±0.5	±0.13	±0.12	±0.5

^a Includes sunlight, eclipse, sun and moon interference.

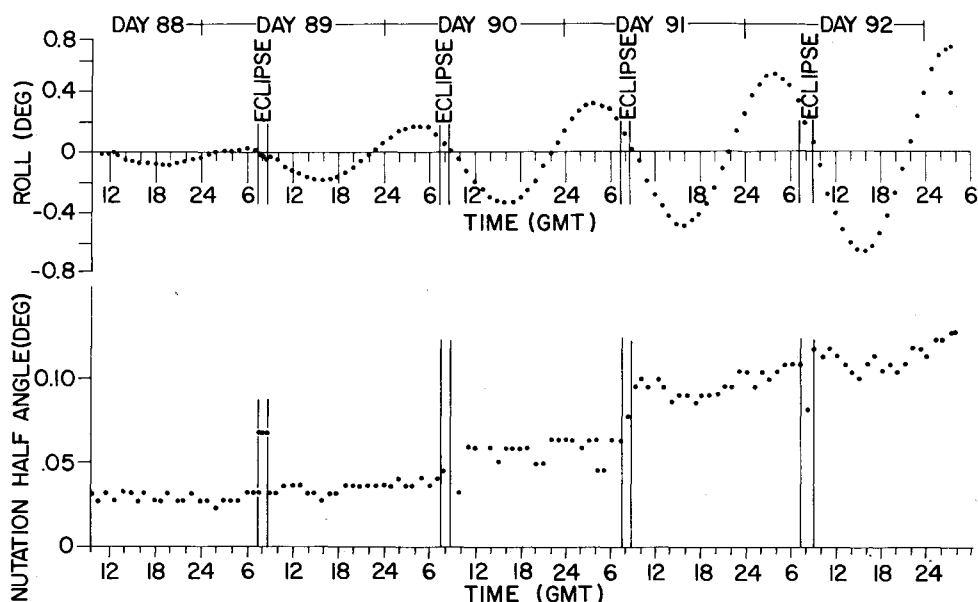


Fig. 16 Average roll angle and nutation half-cone angle vs time, days 88-93, 1976.

NESA - Malfunction and AFP Trip

On day 100, 1976, NESA-A failed to start properly after being turned on. The sensor yielded saturation values of pitch and roll in its temporarily failed state, which resulted in AFP trip. The CWS mode maintained the spacecraft in a safe stable state (a very slow rotation about pitch, and small nutational wobble in roll/yaw) until flight dynamics personnel arrived and were able to reinitiate Earth lock. The AFP trip occurred at about 3:00 a.m. Ottawa time; sun line stabilization followed, and Earth lock-in pitch (NESA-B) was achieved by 6:00 a.m.; completion of reactivation of the onboard system was achieved by about 11:00 a.m.

About five anomalous NESA-A turns-ons have occurred. In this event, procedure is to turn-off immediately and try again. The sensor has always turned-on properly on the second or third attempt with no degradation in performance. The fault is believed to be associated with a mechanical restriction of the scan mirror motion.

AFP has been automatically triggered during the mission, due to anomalous NESA-A behavior. These occurrences have served to demonstrate that the failure-protect concept, based on stored momentum, renders the spacecraft into a safe holding mode during emergencies. Furthermore, one concludes that a constant wheel speed mode is a highly desirable feature for spacecraft of this type.

Attitude Drift and Recapture Test

During days 88-93, 1976, an attitude drift and recapture test event in roll/yaw was conducted. The offset thrusters were inhibited for about 113 h, thus eliminating the active control of roll/yaw and relying on stabilization via gyroscopic stiffness only. At the end of the period, the offset thrusters were enabled, thus reactivating the normal mode of stabilization.

Figure 16 presents the history of an averaged roll angle over one nutation cycle vs time. Averaged roll angle shows the motion of the angular momentum vector, as seen from the spacecraft-fixed roll and yaw axis frame. Figure 16 presents the history of the half-cone angle of nutation. The following observations are made:

1) The angular momentum vector motion is attributable to a solar-induced torque of about 4.6×10^{-7} ft-lb. The Sun elevation angle varies from 2.75-5 deg during this period (March 28-April 3, 1976) and consequently, solar torque is very small.^{3,7}

2) The nutation angle remains constant, except at entry to and exit from eclipse. The nutation will decay in accordance with the amount of structural energy dissipation experienced by the spacecraft. The decay is not observed in time periods of 22 h, which indicates that energy dissipation is negligible.

3) Eclipse entry and exit changes the nutation half-cone angle by as much as 0.04 deg. In some cases, it increases; in others, it decreases. The cause of the change is believed to be thermal shock (thermal-induced structural deformation) experienced by the spacecraft as it transits the shadow-sun boundary. The transit provides a stress and configuration change, which alters the net kinetic energy (but not the angular momentum) of the spacecraft; this is reflected in a change in nutation angle. Analytical modelling and simulation of this type of behavior is not easily done, and has not been attempted.

4) The momentum vector, and hence momentum wheel axis, is misaligned with respect to a normal to the Earth sensor boresight by about 0.05 deg. The evidence of this is that the data shown in Fig. 16 have a nonzero mean value amounting to 0.05 deg.

5) On day 93, the offset thrusters were enabled and the 0.8 deg initial roll error was reduced below 0.06 deg in 20 min,

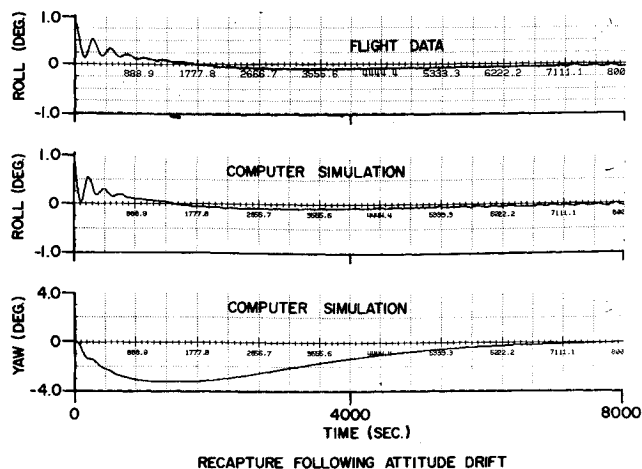


Fig. 17 Comparison of data and simulation results for capture from 0.83 deg roll angle—day 93, 1976.

and the yaw transient became negligible in about 90 min. Data are in accord with the simulation results shown in Fig. 17.

The test demonstrates that system operation with the offset thruster inhibited is a stable mode in sunlight and eclipse for long periods of time. In this instance, roll/yaw attitude was maintained within ± 0.1 deg for more than 24 h.

Pointing Accuracy

Although an absolute reference is not available, conclusions can be drawn regarding pointing accuracy.

At times when the two NESAs are both on, the two telemetered values of pitch or roll differ and change relative to each other with time by as much as 0.15 deg. Data have shown that the changes occur in small steps of 0.02-0.05 deg over 1-2 min intervals, at times of temperature change, such as eclipse entry and exit. The probable cause is thermal deformation associated with the sensors or their mounting bases.

A pointing error summary is given in Table 2.

Structural Flexibility

No control system interactions with structural flexibility or thermal-induced interactions have occurred. The controllers have been designed to accommodate structural flexibility with damping factors greater than 0.004 and measured damping factors are greater than 0.01. More detailed structural dynamics information (measured frequencies and damping factor) are included in Refs. 3 and 4.

Conclusions

The major design parameters (i.e., solar torques, magnetic torque, eclipse-induced transients, misalignment allowance, etc.) for the spacecraft are in accordance with projections made by analysis prior to control system implementation.

The CTS implementation achieves or exceeds performance levels (pointing accuracy, settling time, response to disturbances, fuel consumption, weight, etc.) necessary for efficient satellite communications.

Although the structure has a degree of flexibility,^{3,4} no adverse structural flexibility/control system interaction or solar-induced instabilities are evidenced.

Performance and life data on the components have been favorable to date. An unexpected drag torque variation of the momentum wheel has been observed. A temporary malfunction of one of the scanning Earth sensors has been experienced. An occasional anomalous operation of a pitch thruster has been noted.

Operational methods for momentum dumping, E-W stationkeeping, and sun and moon avoidance, are demonstrated to be successful.

The automatic failure-protect mode of CTS operates as predicted and commands the spacecraft into a safe holding state following loss of Earth lock. Mission experience demonstrates that a safe holding state is valuable and serves as a viable alternate to active backup modes of operation.

Acknowledgment

The authors would like to acknowledge the dedicated efforts of D. Challoner, W. Poteate, and SPAR Aerospace Products Ltd. during the design and implementation phases of the CTS attitude control system. We would also like to thank H. Raine and H. Reynaud for their helpful discussions in reviewing the paper.

References

- ¹Sansevero, V.J., Garfinkel, H., and Archer, S.F., "Flight Performance of the Hydrazine Reaction Control Subsystem for the Communications Technology Satellite," AIAA Paper 76-630, Palo Alto, California, July 1976.
- ²Bassett, D.A., "Ground Controlled Conversion of Communications Technology Satellite (CTS) from Spinning Mode to Three-Axis Stabilized Mode," AIAA Paper 76-1928, San Diego, California, Aug. 1976.
- ³Harrison, T.D., Lang, G.B., Gore, V., Vigneron, F., and Quittner, E., "In-Orbit Characteristics of the Communications Technology Satellite Deployable Solar Array," Eleventh Intersociety Energy Conversion Engineering Conference, Sept. 1976.
- ⁴Vigneron, F.R., "Ground-Test Derived and Flight Values of Damping for a Flexible Spacecraft," ESA SP-117, ESA Symposium on the Dynamics and Control of Non-Rigid Space Vehicles, ESTEC, Noordwijk, Holland.
- ⁵Raine, H.R., "The Communications Technology Satellite Flight Performance," Paper 76-223, International Astronautical Federation 27th Congress, Oct. 1976.
- ⁶Lang, G.B., Trudel, C.P., and Staley, D.A., "CTS Attitude Control Subsystem Analysis Final Report," SPAR-R 626, SPAR Aerospace Products Ltd., Toronto, Canada, Sept. 1974.
- ⁷Vigneron, F.R., McMillan, D.V., and Kettlewell, J.R., "The Attitude Stabilization and Control System for the Communications Technology Satellite," NTC '72 Record, the 1972 National Telecommunications Conference, IEEE Publication 72CHO 601-5-NTC.
- ⁸Millar, R.A. and Vigneron, F.R., "The Effect of Structural Flexibility on the Stability of Pitch for the Communications Technology Satellite," *Proceedings of the Canadian Conference on Automatic Control*, June 1975, University of British Columbia, Vancouver, Canada.
- ⁹Millar, R.A. and Vigneron, F.R., "Attitude Stability and Structural Flexibility in Roll/Yaw for the Communications Technology Satellite," Symposium on Dynamics and Control of Large Flexible Spacecraft, June 1977, Blacksburg, Va.
- ¹⁰Flannery, J. and Alward, J.L., "Seasonal Effects on the Performance of Earth Horizon Sensors," AIAA Paper 76-267, Montreal, Canada, April 1976.
- ¹¹Davis, P., Sutter, C., and Reistad, K., "A Versatile New Reaction Wheel Used on Fleet Sat Com and CTS," EASCON 74, pp. 159-165.